

See discussions, stats, and author profiles for this publication at: <https://www.researchgate.net/publication/257233676>

# Separation of large scale water storage patterns over Iran using GRACE, altimetry and hydrological data

Article in *Remote Sensing of Environment* · September 2013

DOI: 10.1016/j.rse.2013.09.025

CITATIONS

23

READS

384

8 authors, including:



**Ehsan Forootan**

Cardiff University

82 PUBLICATIONS 403 CITATIONS

SEE PROFILE



**Jürgen Kusche**

University of Bonn

198 PUBLICATIONS 1,962 CITATIONS

SEE PROFILE



**Mohammad A. Sharifi**

University of Tehran

139 PUBLICATIONS 432 CITATIONS

SEE PROFILE



**Joseph Awange**

Curtin University

252 PUBLICATIONS 1,107 CITATIONS

SEE PROFILE

Separation of large scale water storage patterns over  
Iran using GRACE, altimetry and hydrological data,  
*Journal of Remote Sensing of Environment*, 140, Pages  
580-595, dx.doi.org/10.1016/j.rse.2013.09.025.

E. Forootan<sup>a</sup>, R. Rietbroek<sup>a</sup>, J. Kusche<sup>a</sup>, M. A. Sharifi<sup>b</sup>, J. L. Awange<sup>c</sup>, M.  
Schmidt<sup>d</sup>, P. Omondi<sup>e</sup>, J. Famiglietti<sup>f</sup>

<sup>a</sup>*Institute of Geodesy and Geoinformation (IGG), Bonn University, Bonn, Germany*

<sup>b</sup>*Surveying and Geomatics Engineering Department, University of Tehran, Iran*

<sup>c</sup>*Western Australian Centre for Geodesy and The Institute for Geoscience Research, Curtin  
University, Perth, Australia*

<sup>d</sup>*German Geodetic Research Institute (DGFI), Munich, Germany*

<sup>e</sup>*IGAD Climate Prediction and Applications Centre (ICPAC), Nairobi, Kenya*

<sup>f</sup>*UC Center for Hydrologic Modeling, University of California, Irvine, CA, USA*

---

## Abstract

Extracting large scale water storage (WS) patterns is essential for understanding the hydrological cycle and improving the water resource management of Iran, a country that is facing challenges of limited water resources. The Gravity Recovery and Climate Experiment (GRACE) mission offers a unique possibility of monitoring total water storage (TWS) changes. An accurate estimation of terrestrial and surface WS changes from GRACE-TWS products, however, requires a proper signal separation procedure. To perform this separation, this study proposes a statistical approach that uses a priori spatial patterns of terrestrial and surface WS changes from a hydrological model and altimetry data. The patterns are then adjusted to GRACE-TWS products using a least squares adjustment (LSA) procedure, thereby making the best use of the available data. For the period of October 2002 to March 2011, monthly GRACE-TWS changes were derived over a broad region encompassing Iran. A priori patterns were derived by decomposing the following auxiliary data into statistically independent components: (i) terrestrial WS change outputs of the Global Land Data Assimilation System (GLDAS); (ii) steric-corrected surface WS changes of the Caspian Sea; (iii) that of the Persian and Oman Gulfs; (iv) WS changes of the Aral Sea; and (v) that of small lakes of the selected region. Finally, the patterns of (i) to (v) were adjusted to GRACE-TWS maps so that their contributions were estimated and GRACE-TWS signals separated. After separation, our re-

---

*Email addresses:* forootan@geod.uni-bonn.de (E. Forootan), roelof@geod.uni-bonn.de (R. Rietbroek), kusche@geod.uni-bonn.de (J. Kusche), sharifi@ut.ac.ir (M. A. Sharifi), J.Awange@curtin.edu.au (J. L. Awange), M. Schmidt: schmidt@dgfi.badw.de (M. Schmidt), philip.omonidi@gmail.com (P. Omondi), jfamigli@uci.edu (J. Famiglietti)

sults indicated that the annual amplitude of WS changes over the Caspian Sea was 152 mm, 101 mm over both the Persian and Oman Gulfs, and 71 mm for the Aral Sea. Since January 2005, terrestrial WS in most parts of Iran, specifically over the center and northwestern parts, exhibited a mass decrease with an average linear rate of  $\sim 15$  mm/yr. The estimated linear trends of groundwater storage for the drought period of 2005 to March 2011, corresponding to the six main basins of Iran: Khazar, Persian and Oman Gulfs, Urmia, Markazi, Hamoon, and Srakhs were -6.7, -6.1, -11.2, -9.1, -3.1, and -4.2 mm/yr, respectively. The estimated results after separation agree fairly well with 256 in-situ piezometric observations.

*Keywords:* GRACE-TWS, Signal separation, Independent components, Terrestrial and surface water storage, Groundwater, Iran

---

## 1. Introduction

Water resource of the Islamic Republic of Iran (Iran) is under pressure due to population growth, urbanization and its related consequences (FAO, 2009). The direct impact of the increasing population ( $\sim 75$  million in 2010) on water resources resulted in increased need for fresh water in populated centers, while its indirect impact was an increase in demand of agricultural land and development of irrigation lands (e.g., Ardakani, 2009). Sarraf et al. (2005) state that the total water resources per capita in Iran plunged by more than 65% since 1960, and a decrease of 16% is expected by 2025. The increased demand for groundwater, on one hand, and the high rate of irrigation and over-exploitation of water resources in some areas on the other hand are also likely to become a serious challenge for future protection of groundwater basins of central and northern Iran (Motagh et al., 2008; Mohammadi-Ghaleni and Ebrahimi, 2011).

Since 90% of Iran is located in arid or semi-arid areas, the direct rainfall is its only water recharge. This means that only 10% of the country receives enough rainfall to meet its need while the other much drier parts are heavily dependent on groundwater. Using Synthetic-Aperture Radar (SAR) data, Motagh et al. (2008) showed a land subsidence related to groundwater storage extractions in the central part of Iran between 1971 and 2001. Combining precipitation data with measured piezometric groundwater levels, Van Camp et al. (2012) pointed out that there is an imbalance between exploitation and precipitation recharge in central Iran, which has resulted in the decline of water storage (WS). Their study, however, was restricted to the Shahrekord aquifer (located at  $\sim [32.3^{\circ}\text{N}]$  and  $[50.9^{\circ}\text{E}]$ ).

Such conditions, therefore, justify the exploration of alternative monitoring tools that can provide reliable information to improve water policies. These are needed in the management of drought and flood related impacts, as well as improving the overall water situation in the region. Among different hydrological parameters, total water storage (TWS), defined as the summation of all water masses in the Earth's storage compartments (atmosphere, surface waters, ground water, etc.), is an important indicator of the water cycle (Güntner,

32 2008). TWS changes can also be used for evaluating the past and present state  
33 of natural resources such as water and fodder, as well as for modeling their  
34 future development within the context of human usage and climate change (see  
35 e.g., [Becker et al., 2010](#); [Grippa et al., 2011](#); [Forootan et al., 2012](#)).

36 For a long time, mapping of terrestrial WS changes mainly relied on piezo-  
37 metric observations, in-situ meteorological measurements, as well as hydrolog-  
38 ical modeling approaches. Although such approaches are very important for  
39 understanding the mechanism of water cycle, they are limited e.g., by data in-  
40 consistencies, spatial and temporal data gaps or instrumental and human errors  
41 and oversights (Rodell et al., 2007). For Iran, specifically, most of the previ-  
42 ous studies focused only on regional water variations, see e.g., Ghandhari and  
43 Alavi-Moghaddam (2011). Using such local studies, it is difficult to assess the  
44 large scale heterogeneity of the terrestrial water cycle, due to the vast climate  
45 and topographic condition of the country (see, e.g., Section 2 and Modarres,  
46 2006). Other studies that looked at the large-scale water variations of Iran were  
47 restricted to the use of hydrological models (e.g., Abbaspour et al., 2009; Noory  
48 et al., 2011).

49 Since March 2002, however, the Gravity Recovery and Climate Experiment  
50 (GRACE) is routinely providing satellite-based estimates of changes in TWS  
51 within the Earth’s system (see e.g., Tapley et al., 2004a,b; Wahr et al., 2004;  
52 Kusche et al., 2012; Famiglietti and Rodell, 2013). GRACE-TWS have been  
53 used to study regional patterns of TWS changes, e.g., over Asia (e.g., Rodell  
54 et al., 2009; [Shum et al., 2011](#); [Schnitzer et al., 2013](#)), Africa (e.g., Awange et  
55 al., 2013; [Becker et al. 2010](#); [Grippa et al., 2011](#)), Australia (e.g., Awange et  
56 al., 2011; [Van Dijk et al., 2011](#); Forootan et al., 2012). On a global scale, TWS  
57 changes are discussed e.g., in [Syed et al. \(2008\)](#), and Forootan and Kusche  
58 (2012). All these studies came to the same conclusion that GRACE-TWS prod-  
59 ucts are suitable for studying large scale WS changes on annual and inter-annual  
60 time scales.

61 Studies which address TWS changes of the regions around Iran include, for  
62 example, the works of Swenson and Wahr (2007) who used satellite altimetry  
63 (Jason1) together with GRACE monthly gravity solutions to analyze the WS  
64 changes of the Caspian Sea from mid 2002 to 2006, and provided a multi-sensor  
65 monitoring of the sea. Avsar and Ustun (2012) showed a downward linear trend  
66 of GRACE derived gravity changes over a region including Turkey and west  
67 of Iran from 2003 to 2010. Studies of Llovel et al. (2010) and Baur et al.  
68 (2013) addressed the basin averaged TWS changes of the Volga River Basin  
69 (located in Russia), as well as Tigris-Euphrates region in Iraq. In the same  
70 region, Longuevergne et al. (2012) evaluated water variations within the Tigris-  
71 Euphrates reservoirs and found a decrease of  $\sim 17 \text{ km}^3$  during the drought  
72 period between 2007 and 2010. In a recent study, Voss et al. (2013) showed that  
73 the pattern of the water loss is extending into the northwestern Iran including  
74 the Urmia Basin (see basin 3 in Fig. 1). They also reported that the strong  
75 decline of water storage was most likely caused by groundwater depletion in  
76 this region between 2003-2009. Our contribution extends these previous studies  
77 by looking at the recent patterns of WS changes (from October 2002 to March

78 2011) over the main basins of Iran.

79 Estimating accurate terrestrial or surface WS changes from GRACE-TWS  
80 products, however, requires a signal separation approach (e.g., Schmidt et al.,  
81 2008; Forootan and Kusche, 2012; Schmeer et al., 2012). This is due to the fact  
82 that: (a) GRACE time-variable gravity field products exhibit correlated errors  
83 at high degrees (e.g., [Swenson and Wahr, 2006](#); [Kusche, 2007](#); [Klees, 2008](#)) that  
84 need to be reduced; and (b) GRACE-TWS products represent a mass integral  
85 which needs to be separated into their compartments. i.e. the mass varia-  
86 tions within Earth’s interior or on its surface or atmosphere. Regarding (a),  
87 it is common to apply a filter before computing TWS changes from GRACE  
88 time-variable gravity products (e.g., [Kusche, 2007](#)). Nevertheless, this filtering  
89 introduces biases in the mass change estimations since the mass anomalies are  
90 smeared out and moved due to the spatial filtering, known as the ‘leakage’ prob-  
91 lem ([Swenson and Wahr 2002](#); [Klees, 2007](#)). [Fenoglio-Marc et al. \(2006; 2012\)](#)  
92 and [Longuevergne et al. \(2010\)](#) show that the leakage is larger for regions where  
93 land meets water reservoirs such as lakes, seas and oceans and also for small  
94 basins. To account for these leakages, most of the previous studies focused on  
95 basin-wide approaches (e.g., [Fenoglio-Marc et al., 2006; 2012](#); [Llovel et al., 2010](#);  
96 [Longuevergne et al., 2010](#); [Baur et al., 2013](#); and [Jensen et al., 2013](#)). However,  
97 due to the vast size of our region of study, and its varying climatic conditions  
98 (see Section 2), it is desirable to implement information extraction methods that  
99 allow the retrieval of spatially varying WS changes. This capability is a feature  
100 that is usually lost when one applies basin-wide averaging methods.

101 Regarding (b), one may assume that the main source of GRACE-TWS vari-  
102 ability consists of the contribution of the terrestrial and surface WS changes  
103 ([Güntner et al., 2007](#)). We assume that the ocean and atmospheric mass vari-  
104 ations have already been removed from GRACE time-variable solutions using  
105 de-aliasing products ([Flechtner, 2007a,b](#)). Although, this procedure in itself  
106 might introduce some errors in TWS estimations (see, e.g., [Duan et al., 2012](#);  
107 [Forootan et al., 2013](#)), that is not considered in this paper. For partitioning  
108 GRACE-TWS, most of the previous studies use altimetry observations to ac-  
109 count for the surface WS changes (e.g., [Swenson and Wahr, 2007](#); [Becker et al.,](#)  
110 [2010](#)) and hydrological models for terrestrial water changes (e.g., [Syed et al.,](#)  
111 [2005](#); [Rodell et al., 2007](#); [Van Dijk, 2011](#); [Van Dijk et al., 2011](#)). Subsequently,  
112 GRACE-TWS signals are compared or reduced with altimetry and/or model de-  
113 rived WS values. The accuracy of the estimation in such approaches might be  
114 limited since, for instance, altimetry observations contain relatively large errors  
115 over inland waters (e.g. [Birkett, 1995](#); [Kouraev et al., 2011](#)) and hydrological  
116 models show limited skill (e.g., [Grippa et al., 2011](#); [Van Dijk, 2011](#)).

117 In this study, however, instead of removing those surface and terrestrial WS  
118 (respectively derived from altimetry and hydrological models) from GRACE-  
119 TWS maps, we use them as a priori information, to introduce the spatial pat-  
120 terns of surface and terrestrial WS changes. Then GRACE-TWS signals are  
121 separated by adjusting the derived spatial patterns to GRACE-TWS maps. For  
122 this means, TWS data within a rectangular box (between  $[23^{\circ}$  to  $48^{\circ}\text{N}]$  and  
123  $[42^{\circ}$  to  $63^{\circ}\text{E}]$ ) that includes Iran, is extracted from each monthly GRACE-TWS

124 map. As mentioned before, the main source of TWS variability, within each  
125 map, consists of the contribution of the terrestrial and surface WS changes  
126 ([Güntner et al., 2007](#)). In our case, the surface water variations are mainly  
127 caused by water reservoirs within the selected box e.g., the Caspian Sea, Per-  
128 sian and Oman Gulfs, Aral Sea as well as other small lakes. Note that the  
129 effect of self-gravitational forces, other than those of surface and terrestrial WS  
130 changes, might be considerable over the region. A discussion can be found in  
131 Appendix B.

132 The higher-order statistical method of independent component analysis (ICA)  
133 ([Foorootan and Kusche, 2012; 2013](#)) is used to identify statistically independent  
134 patterns from (i) monthly WS outputs of the Global Land Data Assimilation  
135 System (GLDAS) model (Rodell et al., 2004) over the selected rectangular box;  
136 (ii) Surface WS changes derived from altimetry observations of Jason1&2 mis-  
137 sions over the Caspian Sea; (iii) sea surface heights (SSH)s in the Persian and  
138 Oman Gulfs after removing steric sea level changes; (iv) surface WS changes  
139 in the Aral Sea; as well as (v) the other main lakes of the selected box. The  
140 derived independent patterns of (i) to (v) were used as known spatial patterns  
141 (base-functions) in a least squares adjustment (LSA) procedure, to separate  
142 GRACE-TWS maps. This procedure gives the opportunity to make the best  
143 use of all available data sets in a LSA framework. A similar argument has been  
144 pointed out e.g., in [Schmeer et al. \(2012\)](#), who used experimental orthogonal  
145 functions of geophysical models in a LSA model for separating global GRACE  
146 integral signals. After separation, besides adjusting the terrestrial WS of (i) to  
147 GRACE-TWS, and the estimation of surface WS changes of the region (ii to  
148 v), for the first time, our study offers changes of the groundwater within the six  
149 main basins of Iran (basins are shown in Fig. 1). Our results are also compared  
150 with in-situ piezometric measurements.

151 The remaining part of the paper is organized as follows: in Section 2, we  
152 briefly describe the study region. The data used in the study is presented in  
153 Section 3. Section 4 outlines the analysis methods, and the results of separation  
154 are presented and discussed in Section 5. Finally, Section 6 concludes the paper  
155 and provides an outlook. The paper also includes two appendices that pro-  
156 vide the results of ICA applied on GLDAS and altimetry derived WS changes  
157 (Appendix A), and the effect of self-gravitation on the results (Appendix B).

## 158 **2. The Study Region**

### 159 *2.1. Geography*

160 Iran with an area of about 1.7 million km<sup>2</sup> lies between latitudes [24° to  
161 40°N] and longitudes [44° to 64°E] (Fig. 1). The landscape of Iran is dominated  
162 by rugged mountain ranges that separate various basins from each other. The  
163 largest mountain chain is that of the Zagros, which runs from the northwest of  
164 the country southwards to the shores of the Persian Gulf and then continues  
165 eastwards along most of the southeastern province. Alborz is the other main

166 mountain chain range that runs from the northwest to the east along the south-  
167 ern edge of the Caspian Sea. Over 50% of the area between the two main chains  
168 are covered by salty swamps of Dasht-e-Kavir and Dasht-e-Lut.

## 169 *2.2. Basins and Climate*

170 According to FAO (2009), there are 6 main catchments in Iran (i.e. Fig.  
171 1) that include, the Central Plateau in the centre (basin 4; Markazi), the Lake  
172 Urmia Basin in the northwest (basin 3), the Persian and Oman Gulf basins in  
173 the west and south (basin 2), the Lake Hamoon Basin in the east (basin 5), the  
174 Kara-Kum Basin in the northeast (basin 6; Sarakhs) and the Caspian Sea Basin  
175 in the north (basin 1; Khazar). All these basins, except the Persian and Oman  
176 Gulf Basin, are interior. The Markazi basin, covering over half of the area of the  
177 country, has less than one third of the total renewable water resources (FAO,  
178 2009). Shapes of the basins, their areas, and the percentage of their renewable  
179 water resources are summarized in Fig. 1.

180 The climate of Iran is quite extreme. Its northern edge is categorized as  
181 subtropical region (Khazar basin in Fig. 1). Whereas the climate of the other  
182 parts, i.e. 90% of the country, ranges from arid to semiarid, with extremely hot  
183 summers in central and the southern coastal regions. The main source of the  
184 input water in Iran is annual precipitation. The highest annual rainfall of 2275  
185 mm has been recorded in Rasht, located near the Caspian Sea. Annual rainfall  
186 is less than 50 mm in the deserts (FAO, 2009).

## 187 *2.3. Main Surface Waters of the Region*

### 188 *The Caspian Sea*

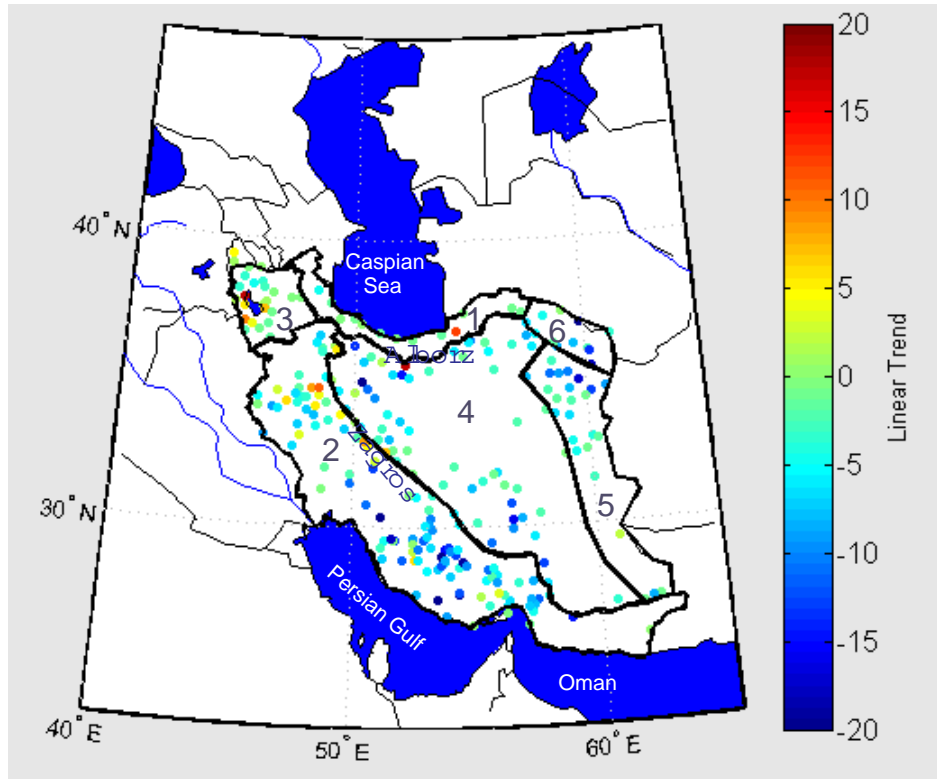
189 The Caspian Sea, with an area of  $\sim 371,000 \text{ km}^2$  is the world's largest inland  
190 water body (Kosarev and Yablonskaya, 1994). Kouraev et al. (2011) provide  
191 a detailed description on the geographical and physical aspects of the Caspian  
192 Sea. The Caspian Sea exhibits considerable fluctuations in its water levels, which  
193 have been the subject of several studies (e.g., Kouraev et al., 2011; Sharifi et  
194 al., 2013). Using a point-wise technique, Sharifi et al. (2013) illustrated that  
195 due to the vast size of Caspian, the varying climatic patterns within the whole  
196 sea, and the large impact of the Volga River, each region of the sea is expected  
197 to have a water level pattern different from the other regions. Their results  
198 indicate that during June 2001 to December 2005 and January 2006 to October  
199 2008, linear rates of level variations are respectively 106 and -161 mm/yr. The  
200 extreme temperature conditions of the sea also contribute to the changing of  
201 the sea level, which exhibits an annual amplitude of  $\sim 20 \text{ mm}$  (e.g., Swenson  
202 and Wahr, 2007).

### 203 *Urmia Lake*

204 Lake Urmia (located in the Urmia Basin of Fig. 1,  $\sim [37.7^\circ\text{N}$  and  $45.31^\circ\text{E}]$ ) is  
205 a salty lake with a surface area of  $\sim 5000 \text{ km}^2$  (year 2000). The area of the lake  
206 is shrinking, which is partly due to the decade-long drought of its watershed  
207 and also due to the construction of 35 dams (since the 1990's) on the rivers



208 which feed the lake. Crétaux et al. (2011) provided altimetry and imagery  
 209 results for Lake Urmia (e.g., [http://www.legos.obs-mip.fr/en/soa/hydrologie/hydroweb/Page\\_2.html](http://www.legos.obs-mip.fr/en/soa/hydrologie/hydroweb/Page_2.html)).  
 210



Major Basins of Iran	Percentage of total area of the country	Percentage of total renewable water resources	Number of Stations	Mean of Linear Trend of 2003-2010
1) Khazar	10	15	24	-6 mm/yr
2) Persian and Oman Gulfs	25	46	91	-5 mm/yr
3) Urmia	3	5	19	-13 mm/yr
4) Markazi	52	29	103	-2.5 mm/yr
5) Hamoon	7	2	12	-1.1 mm/yr
6) Sarakhs	3	3	7	-2.3 mm/yr

Figure 1: An overview of in-situ groundwater stations within the six major basins of Iran. The definition of the basins, their areas and renewable water resource percentages are according to FAO (2009). In-situ observations are provided by the Iranian Water-Resource Research Center. The linear rate of water storage change are computed using a least squares approach, while considering the annual and semi-annual frequencies. The Caspian and Aral Sea as well as the Persian and Oman Gulfs are masked out in blue.



211 *The Persian Gulf and the Gulf of Oman*

212 The Persian Gulf, with a surface area of  $\sim 251,000 \text{ km}^2$ , is a shallow water  
213 body in the south (see Fig. 1). Since the Gulf region is surrounded by arid  
214 land masses, it has strong seasonal and even daily air temperature fluctuations.  
215 Air temperature can drop to  $0^\circ\text{C}$  in winter and reach up to  $50^\circ\text{C}$  in summer  
216 (Kampf and Sadrinasab, 2006), which can contribute to the level fluctuations.  
217 Long-term observations of sea level also shows a rise at the head of the Persian  
218 Gulf, located in the Tigris-Euphrates delta of southern Iraq and the adjacent  
219 regions of southwestern Iran. Lambeck et al. (2002) linked this rise to post  
220 glacial rebound.

221 The Gulf of Oman connects the Arabian Sea to the Persian Gulf via the strait  
222 of Hormuz. The waters of the Gulf of Oman have more oceanic characteristics  
223 than those of the Persian Gulf. However, this does not make the fluctuation of  
224 the Gulf greater than the Persian Gulf. Hydrology and circulation aspects of  
225 the Oman Gulf are discussed e.g., in Pous et al. (2004).

### 226 3. Data

227 Four main datasets for the period of 2002 to 2011 were used in this study.  
228 These are (a) monthly TWS variations derived from GRACE, (b) surface WS  
229 changes derived from satellite altimetry observations, (c) terrestrial WS changes  
230 from GLDAS, and (d) 256 in-situ piezometric observations covering the six main  
231 basins of Iran. In addition, maps of sea surface temperature (Reynolds et al.,  
232 2002) and steric sea level (Ishii and Kimoto, 2009) variations are also used to  
233 reduce the contribution of temperature and salinity changes from altimetric  
234 SSHs, while converting them to surface WS changes. Note that surface WS is  
235 commonly called equivalent water height (EWH) in other studies.

#### 236 3.1. GRACE

237 GRACE, a joint German/USA satellite project, was launched in March 2002  
238 to detect mass variations within the Earth's system. In this work, we examined  
239 monthly GFZ release 04 gravity field solutions provided by the German Research  
240 Centre for Geosciences (GFZ) (Flechtner, 2007b). The data was computed up  
241 to degree and order 120 and cover the period from October 2002 to March 2011.  
242 GRACE degree 1 coefficients have been augmented by the results of Rietbroek  
243 et al. (2009) in order to include the variation of the Earth's center of surface  
244 figure with respect to the Earth's centre of mass, in which GRACE products  
245 have been computed. We also replaced the zonal degree 2 spherical harmonic  
246 coefficients ( $C_{20}$ ) by values obtained from satellite laser ranging (SLR) (Cheng  
247 and Tapley, 2004), which were obtained from the GRACE Tellus Team website  
248 ([grace.jpl.nasa.gov](http://grace.jpl.nasa.gov)).

249 GRACE time-variable products contain correlated errors, manifesting itself  
250 as a striping pattern (Kusche, 2007). In order to remove the stripes, we applied  
251 the de-correlation filter of DDK2 (Kusche et al., 2009) to the GFZ solutions.  
252 The choice of the DDK2 filter, which is an anisotropic filter, arises from the

253 consistent results with respect to the outputs of hydrological models (Werth et  
254 al., 2009). Before computing monthly TWS fields, residual gravity field solutions  
255 with respect to the temporal average over the study period were computed. The  
256 residual coefficients were then transformed into  $0.5^\circ \times 0.5^\circ$  TWS maps using the  
257 approach in Wahr et al. (1998). A rectangular box between ( $[23^\circ$  to  $48^\circ\text{N}]$  and  
258  $[42^\circ$  to  $63^\circ\text{E}]$ ) was then extracted from the monthly TWS grids. For the region  
259 of interest, the gridded Root-Mean-Square (RMS) of the GRACE-TWS signals  
260 is shown in Fig. 2,A. Strong anomalies are visible over the Caspian Sea, Lake  
261 Urmia, as well as over parts of the Zagros and Alborz mountains. The large  
262 RMS of the signal over the Caspian Sea and the mountains are due to the strong  
263 seasonality of TWS changes. Over Urmia, the strength of the GRACE-derived  
264 storage signal is mainly due to the water loss of the lake (see e.g., Voss et al.,  
265 2013).

### 266 3.2. Altimetry Data

267 We used monthly gridded altimetry data over the rectangular region men-  
268 tioned above (including the Caspian Sea, the Aral Sea, the Persian and Oman  
269 Gulfs, and Urmia Lake as well as other small lakes and reservoirs), cover-  
270 ing 2002 to 2011.3. Sea surface heights (SSH)s were originally produced by  
271 AVISO and provided through NOAA ERDDAP (the Environmental Research  
272 Division’s Data Access Program program, see [http://coastwatch.pfeg.noaa.gov/erddap/griddap/noaa\\_pifsc\\_9c36\\_df47\\_3dd4.html](http://coastwatch.pfeg.noaa.gov/erddap/griddap/noaa_pifsc_9c36_df47_3dd4.html)). The RMS of the altimetry  
273 signals is shown in Fig. 2,B. For the Caspian Sea, which has the dominant im-  
274 pact on the GRACE-TWS signals over the region, we compared NOAA’s SSH  
275 with the gridded results of Sharifi et al. (2013), and obtained a correlation of  
276 0.91 for the period of 2002 to 2010.

277  
278 Water level fluctuations derived from altimetry can be compared to GRACE  
279 results, when they are corrected for the so called steric or volumetric height vari-  
280 ations caused by temperature and salinity changes (Chambers, 2006). From the  
281 areas that contain surface water in this study, the levels of the Caspian Sea  
282 and the Persian and Oman Gulfs exhibit a considerable steric component. We  
283 used monthly steric sea level changes of Ishii and Kimoto (2009) to convert  
284 SSH of the Persian and Oman Gulfs to surface WS changes. Since Ishii and  
285 Kimoto (2009)’s study does not cover the Caspian Sea, we followed the ap-  
286 proach of Swenson and Wahr (2007) by using SST (sea surface temperature)  
287 data and taking a conversion factor of 8.43 mm/yr to convert them to steric  
288 sea level changes over the Caspian Sea. The SST data, used here, were recon-  
289 structed Reynolds et al. (2002) SST maps obtained from the United States (US)  
290 National Oceanic and Atmospheric Administration (NOAA) official website  
291 (<http://www.esrl.noaa.gov/psd/data/gridded/data.ncep.oisst.v2.html>). Each  
292 map of SSH (after reducing the steric part) was filtered using the same DDK2  
293 filter as applied to the GRACE-TWS maps. After applying the DDK2 filter on  
294 surface WS data, the mean damping ratio of the filtered data to the original  
295 values was  $\sim 0.71$ .

296 *3.3. GLDAS Model*

297 The GLDAS hydrological model integrates a large quantity of observed  
 298 data and modeling concepts (Rodell et al., 2004) to produce a global hydro-  
 299 logical model. GLDAS terrestrial WS data for the period of study were ob-  
 300 tained from the Goddard Earth Sciences Data and Information Services Center  
 301 (<http://grace.jpl.nasa.gov/data/gldas/>). Consequently, terrestrial WS consid-  
 302 ered here constitutes of total column soil moisture (TSM), Snow Water Equiv-  
 303 alent (SWE) and Canopy Water Storage (CWS). Groundwater storage changes  
 304 are not represented in the GLDAS model simulations. As a result, our a priori  
 305 pattern of the terrestrial storage partitioning is limited, and might not include  
 306 a complete description of the lateral and vertical distribution of water storage  
 307 up to the surface (see e.g., Rodell and Famiglietti, 2001; Syed et al., 2008). The  
 308 GLDAS-WS data were filtered by the same DDK2 filter in order to match the  
 309 signal content of the GRACE-TWS fields. The RMS of GLDAS data for the  
 310 mentioned rectangular box is shown in Fig. 2,C. The results show strong signals  
 311 over the northwest of the country and over the Zagros and Alborz mountains.  
 312 The strength of the signal is due to the strong annual variability of TWS over  
 313 these regions. We compared the mean magnitude of the DDK2-filtered GLDAS  
 314 data with its original values over the region and found a damping ratio of  $\sim 0.83$   
 315 due to the filter.

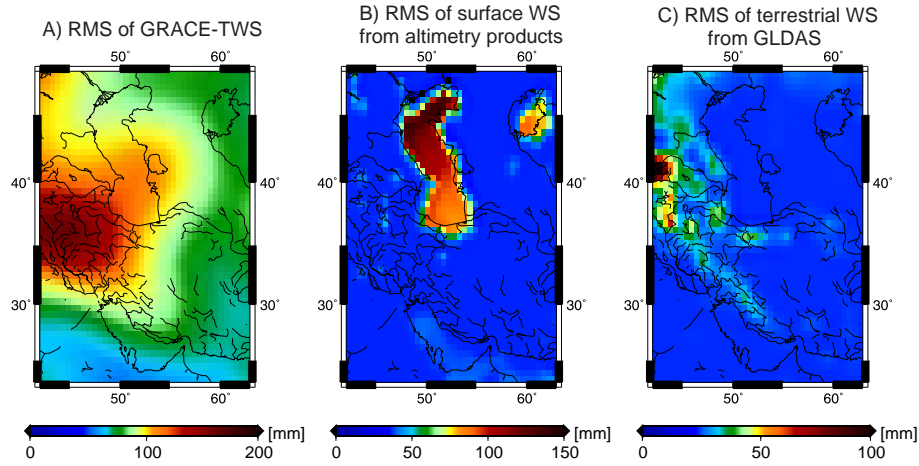


Figure 2: The signal strength (RMS) of the three main data sets used in this study after smoothing using Kusche et al. (2009)’s DDK2 filter; (A) GRACE-TWS data, (B) surface WS from altimetry data and (C) terrestrial WS output of the GLDAS model.

316 *3.4. In-situ Piezometric Measurements*

317 This study used in-situ groundwater observations of 256 selected piezometric  
 318 stations of the Iranian Water-resource Research Center, of which 24, 91, 19, 103,  
 319 12 and 7 stations are located in the basins one to six of Fig. 1, respectively. The  
 320 observations cover the period 2003 to 2010 and have been tested for their quality

321 in terms of outliers and possible biases. The location of the stations and their  
 322 computed linear trends for 2003 to 2010 are shown in Fig. 1. In agreement with  
 323 the other data, most parts of Iran exhibited a WS decline during the mentioned  
 324 period. Note that, there jumps exist in the in-situ time series as a result of  
 325 water network changes. Their impact on the computed trends will be addressed  
 326 in Section 5.2.

#### 327 4. Methodology

328 Monthly GRACE-TWS maps, used in this study (ocean and atmospheric  
 329 mass variations are already removed), reflect an integral measure of the com-  
 330 bined effect of terrestrial WS changes of land hydrology ( $H$ ), and surface WS  
 331 changes of seas, lakes and reservoirs ( $R$ ). Assuming that GRACE-TWS fields  
 332 are stored in a matrix  $\mathbf{T} = \mathbf{T}(s, t)$ , where  $t$  is the time, and  $s$  stands for spa-  
 333 tial coordinate (grid points).  $\mathbf{T}$  can be factorized into spatial and temporal  
 334 components (Schmeer et al., 2012) as

$$\mathbf{T} = \mathbf{C}_H \mathbf{A}_H^T + \mathbf{C}_R \mathbf{A}_R^T, \quad (1)$$

335 where  $\mathbf{C}_{H/R} = \mathbf{C}_{H/R}(t)$  and  $\mathbf{A}_{H/R} = \mathbf{A}_{H/R}(s)$  are respectively the temporal  
 336 and spatial patterns (base-functions). We used  $H$  and  $R$  as subindices to show  
 337 the base-functions that are computed from terrestrial WS ( $H$ ) and surface WS  
 338 ( $R$ ). In Eq. 1,  $\mathbf{C}_H$  contains zero over the gridpoints of surface water and  $\mathbf{C}_R$   
 339 contains zeros over the land.

340 In Eq. 1, once either of  $\mathbf{C}_{H/R}(t)$  or  $\mathbf{A}_{H/R}(s)$  is determined, the other com-  
 341 ponent can be computed by solving a LSA. Schmeer et al. (2012) used a similar  
 342 approach for separating global GRACE-TWS integral into its atmospheric, hy-  
 343 drologic and oceanic contributors. Their study suggests the application of a  
 344 statistical decomposition method on the data/model of each compartment to  
 345 compute the required base-functions of Eq. 1. Accordingly, we follow their  
 346 approach and use steric corrected SSHs and the WS output from the GLDAS  
 347 model as described in Section 3 to compute the required  $\mathbf{C}_{H/R}$  and  $\mathbf{A}_{H/R}$ .

348 ICA, an extension of the second-order statistical method of principal compo-  
 349 nent analysis (PCA) (Preisendorfer, 1988), allows the extraction of statistically  
 350 independent patterns from spatio-temporal data sets (Cardoso and Souloumiac,  
 351 1993). Applications of ICA for filtering (Frappart et al., 2010) and decomposi-  
 352 tion of GRACE-TWS are discussed e.g., in Forootan and Kusche (2012; 2013)  
 353 and Forootan et al. (2012). Of the two alternative ways of applying ICA, in  
 354 which either temporally independent components or spatially independent com-  
 355 ponents are constructed (Forootan and Kusche, 2012), we used temporal ICA.  
 356 The motivation of this selection was based on the intentions of the study, which  
 357 focuses on signals which have distinct temporal behaviour (e.g., seasonal and  
 358 trend of water changes). The temporal ICA method is simply called ICA in this  
 359 paper, and the decomposition of the centered (temporal mean removed) time  
 360 series of  $\mathbf{H}$  and  $\mathbf{R}$  is written as

$$\mathbf{H} = \bar{\mathbf{P}}_H \hat{\mathbf{R}}_H \hat{\mathbf{R}}_H^T \mathbf{E}_H^T = \mathbf{C}_H \mathbf{A}_H^T, \quad (2)$$

361 and

$$\mathbf{R} = \bar{\mathbf{P}}_R \hat{\mathbf{R}}_R \hat{\mathbf{R}}_R^T \mathbf{E}_R^T = \mathbf{C}_R \mathbf{A}_R^T. \quad (3)$$

362 As stated in Forootan and Kusche (2012),  $\bar{\mathbf{P}}_{H/R}$  and  $\mathbf{E}_{H/R}$  contain orthogonal  
 363 components in their columns that are derived by applying PCA on the centered  
 364 data sets of  $\mathbf{H}$  and  $\mathbf{R}$  (Preisendorfer, 1988). In Eqs. 2 and 3,  $T$  is a transpose  
 365 operator,  $\bar{\mathbf{P}}_{H/R}$  is normalized (i.e.  $\bar{\mathbf{P}}_{H/R} \bar{\mathbf{P}}_{H/R}^T = \mathbf{I}$ ),  $\hat{\mathbf{R}}_{H/R}$  is an optimum  
 366 rotation matrix that rotates the temporal components of  $\bar{\mathbf{P}}_{H/R}$  to make them  
 367 temporally as mutually independent as possible (Forootan and Kusche, 2012).

368 As a result of the temporal ICA decomposition,  $\mathbf{C}_{H/R} = \bar{\mathbf{P}}_{H/R} \hat{\mathbf{R}}_{H/R}$  con-  
 369 tains statistically mutually independent temporal components.  $\mathbf{A}_{H/R} = \bar{\mathbf{E}}_{H/R} \hat{\mathbf{R}}_{H/R}$   
 370 stores their corresponding spatial maps, that are still orthogonal.  $\mathbf{A}_{H/R}$ , there-  
 371 fore, will be used in Eq. 1 as known spatial patterns and a new temporal  
 372 expansions of  $\hat{\mathbf{C}}_{H/R}$  will be computed using the LSA approach (e.g., Koch,  
 373 1988),

$$[\hat{\mathbf{C}}_H \hat{\mathbf{C}}_R]^T = \left[ [\mathbf{A}_H \mathbf{A}_R]^T [\mathbf{A}_H \mathbf{A}_R] \right]^{-1} [\mathbf{A}_H \mathbf{A}_R]^T \mathbf{T}^T. \quad (4)$$

374 In Eq. 4,  $\hat{\mathbf{C}}_{H/R}$  contains adjusted temporal components over the land and  
 375 surface waters and  $\mathbf{T}$  contains GRACE-TWS observations. Then,  $\hat{\mathbf{C}}_H$  and  $\hat{\mathbf{C}}_R$   
 376 can be respectively replaced in Eqs. 2 and 3 to reconstruct terrestrial WS  
 377 changes over the land and surface WS changes.

## 378 5. Numerical Results

### 379 5.1. Comparison of GRACE and altimetry

380 From Fig. 2,A, the strongest variability during 2002-2011 detected by GRACE  
 381 is concentrated over Urmia Lake and the Caspian Sea. Before implementing the  
 382 separation approach described in Section 4, we first compared the averaged vol-  
 383 ume variations of Urmia and the Caspian Sea derived from GRACE with those  
 384 of satellite altimetry. For deriving the time series of the Urmia Basin, we took  
 385 the boundary of basin (3) in Fig. 1 as our reference. A basin-averaged TWS  
 386 was computed for Urmia Lake using a similar approach to that of Swenson and  
 387 Wahr (2007), which is the dash-black line in Fig. 3,A. Then, the contribution  
 388 of terrestrial WS surrounding Urmia Lake was removed from GRACE-TWS  
 389 using GLDAS data, which is shown as the solid-black line in Fig. 3,A. Our re-  
 390 sult of surface WS changes from GRACE is comparable, in terms of cycles and  
 391 trend, with those of Crétaux et al. (2011) for Lake Urmia (the solid-gray line in  
 392 Fig. 3,A), derived from altimetry and imagery products (<http://www.legos.obs->  
 393 [mip.fr/soa/hydrologie/hydroweb/](http://www.legos.obs-mip.fr/soa/hydrologie/hydroweb/StationsVirtuelles/SV_Lakes/Urmia.html) StationsVirtuelles/SV\_Lakes/Urmia.html).

394 WS change of the Caspian Sea from GRACE products is shown by the solid-  
 395 black line in Fig. 3,B. For computing the averaged surface WS changes over the  
 396 Caspian Sea, the average value of steric corrected SSHs was multiplied by the  
 397 surface area of the sea and is shown by the solid-gray line in Fig. 3,B. The  
 398 correlation coefficient between the two curves is 0.81, at 95% confidence level,  
 399 indicating a good agreement. However, in some years (e.g., 2004 and 2008), there  
 400 are observable differences between the estimated amplitude of the annual WS  
 401 signal from GRACE and altimetry. This could be due to the steric correction  
 402 or due to the errors in altimetry data itself. Such observed inconsistencies  
 403 motivated the introduced approach for separating GRACE-TWS signals.

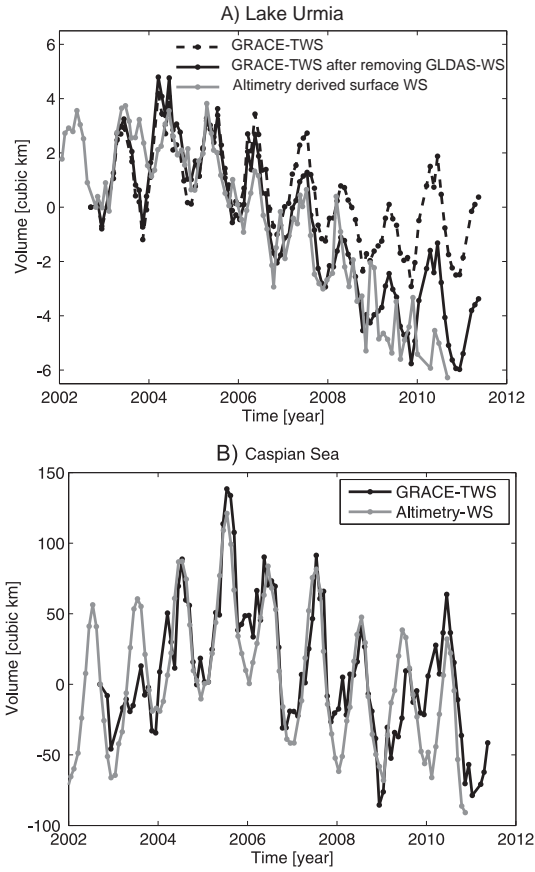


Figure 3: Surface WS changes derived from GRACE and altimetry data, for (A) Lake Urmia and (B) the Caspian Sea. For computing the volume (y-axis), the mean surface area of the Caspian Sea and Urmia Lake (Section 2.3) are multiplied by the mean columns WS changes derived from GRACE and altimetry. During the computations, the shrinking area of Lake Urmia is also taken into account (see also Crétaux et al., 2011).

404 *5.2. Separation (Adjustment) Results*

405 The RMS of GRACE-TWS signals in Fig. 2,A clearly demonstrates the  
406 leakage problem. For instance, a part of the Caspian Sea’s WS leaked into its  
407 surrounding terrestrial signal or vice versa. In order to separate GRACE-TWS  
408 changes, we first extracted independent components of WS changes from altime-  
409 try and GLDAS outputs. The results are shown and described in Figs. A1, A2,  
410 A3, A4 and A5 of Appendix A. The spatial patterns of the mentioned figures  
411 were postulated as known patterns in Eq. 4. We also added four other indepen-  
412 dent components from GLDAS data to Eq. 4. Note that, in order to restrict the  
413 length of the paper, spatial patterns of IC3 to IC6 are not shown in Appendix  
414 A. The adjusted temporal patterns of surface and terrestrial WS changes are  
415 computed using Eq. 4 and are shown in Figs. 4 and 5, respectively. In this  
416 paper, the temporal components are scaled by their standard deviations to be  
417 unit-less. Spatial patterns of the figures in Appendix A and B are scaled by the  
418 standard deviations of their corresponding temporal components to represent  
419 anomaly maps of WS in millimeter.

420 From the annual patterns of surface WS changes, i.e. Fig. 4, A, C, E and  
421 F, the amplitude of the adjusted signals are comparable to those of altime-  
422 try derived surface WS (EWH) changes. Comparing the adjusted inter-annual  
423 changes of surface WS changes (the black lines in Fig. 4,B and D) to their  
424 altimetry-derived estimates (the red lines in Fig. 4,B and D) shows that the  
425 adjusted values (i.e. coming from GRACE products) are smoother compared  
426 to the altimetry results. This is also true for the annual component of the Aral  
427 Sea (compare the red and black lines in Fig. 4,E). Investigating the reason for  
428 this difference may be the subject of future research.

429 From the adjusted results, we estimate the amplitude of annual surface WS  
430 changes of the Caspian Sea to be  $150\text{ mm}$ , whereas amplitudes of  $101\text{ mm}$  and  
431  $71\text{ mm}$  are obtained for the Persian and Oman Gulfs, respectively. Fig. 4, E  
432 indicates a negative linear trend of  $\sim 20\text{ mm/yr}$  during 2002 to 2011 over the  
433 Aral Sea.

434 IC1 in Fig. 5,A compares the adjusted value of annual terrestrial WS changes  
435 with the WS output of GLDAS. Although, the phase of the signal is comparable,  
436 the amplitudes of the signal differ over the years. For instance, an attenuation  
437 of the annual amplitudes in the years 2008 and 2009, derived from GRACE  
438 (the red line in the temporal pattern of IC1) could be related to the prolonged  
439 drought condition over Iran (Shean, 2008). This impact is not fully reflected in  
440 the GLDAS outputs (the black line in Fig. 5,A). IC2 of GLDAS (the black line  
441 in Fig. 5,B) shows an overall decline of terrestrial WS changes mainly over the  
442 central and north-western parts of Iran (see the spatial map of IC2 in Fig. A5).  
443 The adjusted value of IC2 (the red line in Fig. 5,B) shows that the drought  
444 trend actually starts from 2005. The adjusted results are more consistent with  
445 the drought behaviour we found for the small lakes of the country and also in-  
446 situ observations, with all showing a decline after 2005. We estimate an average  
447 decline of  $15\text{ mm/yr}$  water column during 2005 to 2011 over central Iran.



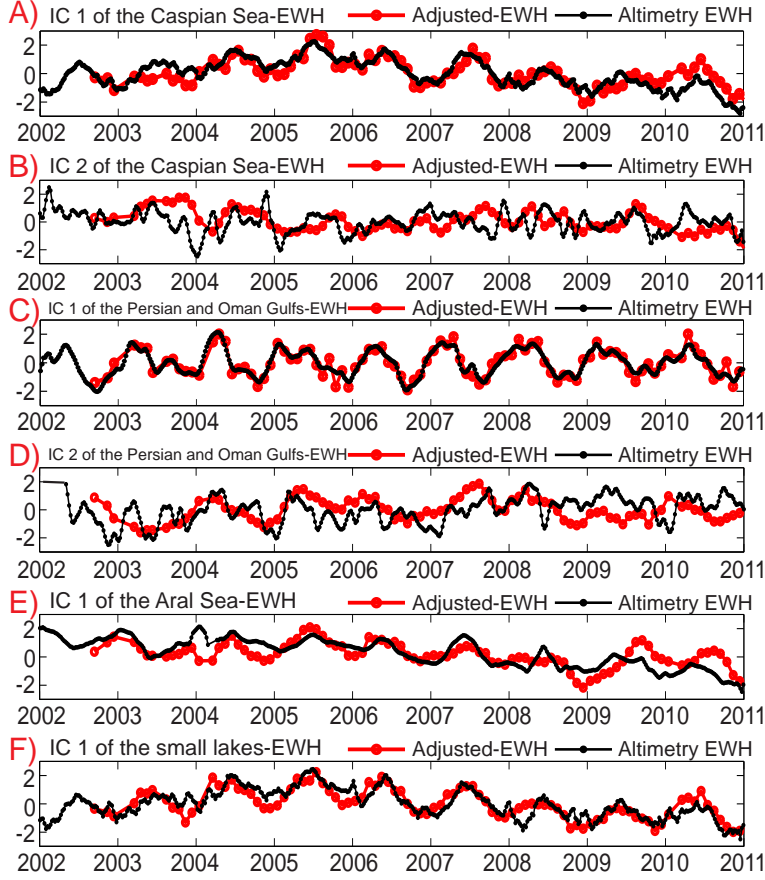


Figure 4: An overview of the adjusted and altimetry derived surface WS changes, shown here in equivalent water height (EWH). The red lines are derived using the LSA method of Section 4 and the black lines are derived from the ICA decomposition of altimetry derived surface WS changes (see Appendix A). (A,B) the first two independent components of the Caspian Sea; (C,D) the first two independent components of the Persian and Oman Gulfs; (E) the first independent component of the Aral Sea; and (F) the first independent component of the small lakes. The temporal patterns are unit-less. The corresponding spatial patterns of (A,B) are shown in Fig. A1; those of (C,D) in Fig. A2; the spatial pattern of (E) in Fig. A3; and that of (F) in Fig. A4. The independent modes are ordered with respect to the variance fraction they represent.

448 *5.3. Comparison of the Adjusted Results with In-situ Observations*

449 Once the signals of the surface and terrestrial WS changes have been sepa-  
 450 rated and their amplitudes are adjusted to the GRACE observations, we use the  
 451 spatial base-functions derived from GLDAS (i.e. spatial maps of Fig. A5 and  
 452 4 other maps that are not shown in the paper) along with their corresponding  
 453 adjusted temporal values (the red lines in Fig. 5 and 4 others) in Eq. 2 to re-  
 454 construct terrestrial WS changes over Iran. In Eq. 2, the spatial maps stored in  
 455  $\mathbf{A}_H$  and  $\mathbf{C}_H$  contain the adjusted temporal components. The RMS and linear

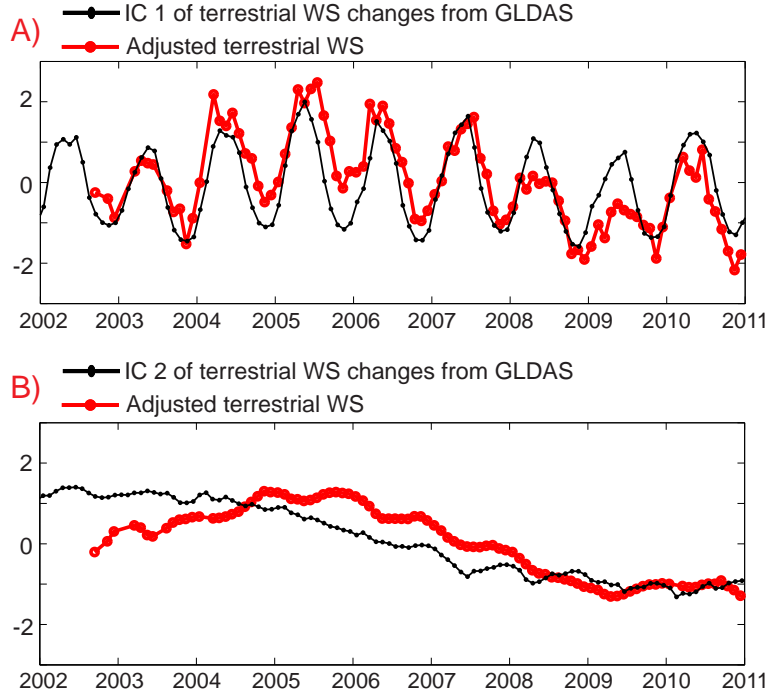


Figure 5: An overview of the main temporal variations of terrestrial WS changes over Iran. The red lines are derived using the LSA method of Section 4 and the black lines are derived from ICA decomposition of GLDAS terrestrial WS changes. (A) corresponds to the first leading independent component, and (B) to the second independent component. The temporal patterns are unit-less and their corresponding spatial patterns are shown in Fig. A5.

456 trends of the reconstructed signals are shown in Fig. 6,A and B, respectively.  
 457 The RMS shows that the separation was successful, where for example, the leak-  
 458 age caused by the Caspian Sea signal is removed (compare Fig. 6,A with Fig.  
 459 2,A). The linear trends (Fig. 6,B) show a decline in most parts of the country  
 460 including the northwest, central, as well as over the Zagros chain.

461 We removed the above reconstructed results from GRACE-TWS maps and  
 462 compared the results with available in-situ groundwater observations. Before,  
 463 comparison, each month of the available stations was first smoothed using a  
 464 Gaussian filter of 400 km radius (Jekeli, 1981). The radius of 400 km was se-  
 465 lected to be approximately consistent with the DDK2 filter applied to GRACE-  
 466 TWS data. We compared the magnitude of the basin averages of the filtered  
 467 in-situ observations with those we derived from the original values (in Fig. 1).  
 468 We found a mean damping factor of  $\sim 0.71$ , which shows the impact of the  
 469 GRACE-like post processing on the true in-situ signals. A comparison of the  
 470 results is shown in Fig. 7. The basin averages derived from both in-situ and  
 471 satellite observations are consistent in terms of the seasonal peaks and phases.  
 472 The linear rates of the water storage changes are depicted in Fig. 7 (dash lines).

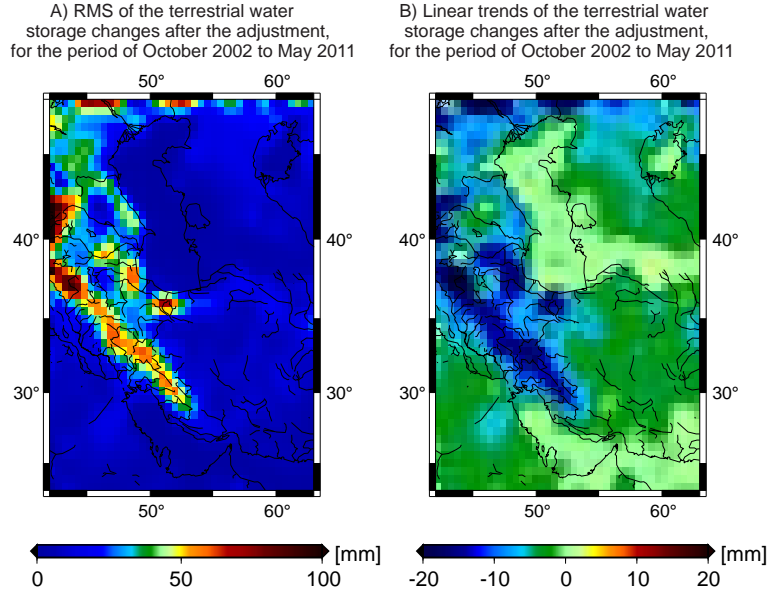


Figure 6: An overview of the reconstructed terrestrial water storage changes over Iran. (A) the RMS of the terrestrial TWS changes after adjusting GRACE-TWS changes (cf. Fig. 2,A) to the base-functions of GLDAS-derived terrestrial WS changes, and (B) the linear trends of the signal in (A).

Basins:	Khazar (Basin 1)	Gulfs (Basin 2)	Urmia (Basin 3)	Markazi (Basin 4)	Hamoon (Basin 5)	Sarakhs (Basin 6)
Groundwater rate of 2003-2005 [mm/yr]:	8.6	5.1	8.5	2.5	1.3	3.7
Groundwater rate of 2005-2011 [mm/yr]:	-6.7	-6.1	-11.2	-9.1	-3.1	-4.2

Table 1: Basin average trends of groundwater variations over the six main basins of Iran derived from GRACE products.

473 As the figure illustrates, in most of the basins, GRACE derived basin averages  
 474 tend to show steeper slopes compared to the in-situ observations. Part of this  
 475 inconsistency might be the result of network changes in a number of stations.  
 476 We removed those stations from our basin average computations and the new  
 477 results turned out to be more consistent with that of GRACE (solid gray lines).  
 478 The other part of inconsistency might be due to our limited knowledge about  
 479 the porosity parameters used for converting piezometer observations to storage  
 480 values, which can be quite large for some basins (see e.g., Jiménez-Martínez et  
 481 al., 2013). Further research, e.g., involving permanent GPS stations, needs to  
 482 be undertaken to address the problem over the selected region. The results of  
 483 GRACE-derived groundwater rates are summarized in Table 1.

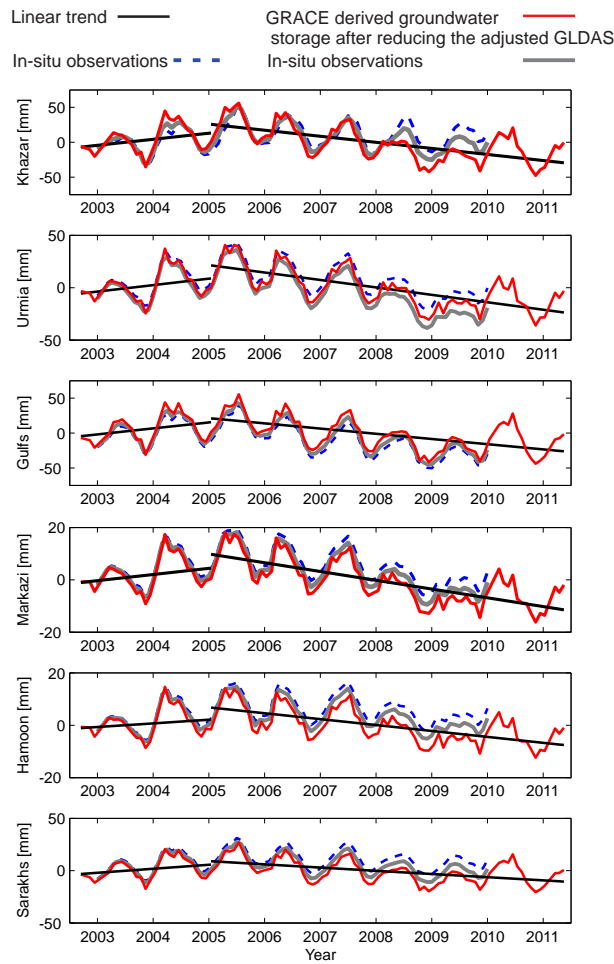


Figure 7: Basin averages of groundwater changes over the six major basins of Iran. The red lines are basin averages after removing the adjusted terrestrial and surface WS changes from GRACE-TWS. The blue dashed lines are derived from in-situ piezometric observations that are located in each basins, respectively. Solid gray lines are derived from the stations, that do not exhibit network changes. Linear trends are shown by the black lines and their rates are reported in Table 1.

## 484 6. Conclusion and Outlooks

485 The water resources in Iran as a part of the Middle-East region are inherently  
 486 scarce as a result of naturally arid climatic conditions. Population increase and  
 487 economic growth have spurred higher demands for the limited water resources  
 488 (FAO, 2009). Therefore, it is desirable to develop monitoring and analysis tools  
 489 to aid understanding the hydrological cycle of the region. In this context, this  
 490 study investigated large scale GRACE-TWS pattern changes over a rectangular  
 491 region that included Iran for the period from October 2002 to March 2011. The  
 492 extracted patterns are important since GRACE-TWS changes represent integral  
 493 measurements of water in the entire region. Spatio-temporal changes of TWS,  
 494 therefore, may be used to study natural and man-made impacts on the regional  
 495 climate.

496 In order to deal with the leakage problem of GRACE products and also

497 to separate terrestrial from surface WS changes, a least squares adjustment  
498 approach was applied on the ICA-decomposed terrestrial and surface WS varia-  
499 tions respectively from GLDAS and altimetry WS outputs. The applied method,  
500 only relies on the ICA-derived spatial patterns of the hydrological model and  
501 altimetry observations, which remain invariant in the adjustment. In the ad-  
502 justment step, the temporal components are estimated from GRACE-TWS data  
503 (Section 5.2). Adjusted terrestrial WS over Iran showed an overall declining  
504 trend over the country (Fig. 6,B). In Section 5.3, we demonstrated that the es-  
505 timated groundwater storages are in a good agreement with in-situ piezometric  
506 observations. Furthermore, for the first time, this study offers GRACE-derived  
507 basin averaged groundwater changes for the six main basins of Iran (basins are  
508 selected according to FAO, 2009). Our estimates of the linear trends of WS  
509 changes for the period of 2003 to 2005 and the drought period of 2005 to 2011.3  
510 are shown in Table 1. In view of the low availability of renewable water resources  
511 in all the basins, in particular, the Markazi and Urmia basins, the results may  
512 be an important incentive for the water resource management of Iran. Note  
513 that the area of some of our processed basins, for instance Urmia and Sarakhs,  
514 are relatively small and might not meet the nominal resolution of the GRACE-  
515 TWS products. However, the strong WS signal of the basins and the proposed  
516 optimal processing method allowed retrieval of water storage variations.

517 At the root of the presented separation procedure lies the ICA-decomposition  
518 of the GLDAS and altimetry outputs. Such decompositions contain errors as a  
519 result of the short length of observations, as well as the errors of observations  
520 themselves. Including those errors in the least squares procedure may poten-  
521 tially improve the results but falls outside the scope of the current research. The  
522 performed separation approach has the potential to be improved by adding extra  
523 information on the patterns of water storage variations over the Mesopotamia  
524 region, which covers the Tigris/Euphrates River system, Lake Van etc., (see  
525 e.g., Voss et al., 2013). The contribution of such base-functions in the inversion  
526 will, however, be marginal and concentrated over the basins located at the west  
527 part of the country (i.e. basins 2 and 3). The relationship between WS changes  
528 in the six major basins of Iran and climate variability such as decadal rainfall  
529 anomalies and large scale ocean-atmospheric patterns of e.g., the El Niño South-  
530 ern Oscillation phenomenon might be helpful for understanding the water cycle  
531 of the region.

## 532 **Acknowledgement**

533 The authors thank the editor M. Bauer and the anonymous reviewer for  
534 the helpful remarks, which improved the manuscript considerably. E. Forootan  
535 and J. Kusche are grateful for the financial support provided by the German  
536 Research Foundation (DFG) under the project BAYES-G. E. Forootan thanks  
537 L. Moxey (the Operations Manager of NOAA OceanWatch - Central Pacific)  
538 for the fruitful discussions on altimetry of the Caspian Sea. He also thanks L.  
539 Longuevergne (Université de Rennes1) for his useful comments on the performed  
540 investigations. The authors also thank Y. Hemmati (Iranian Water-resource

541 Research Center) for providing the in-situ observations. We are grateful for the  
542 satellite and model data used in this study. This is a TIGeR Publication no.  
543 491.

544 Abbaspour, K.C., Faramarzi, M., Seyed Ghasemi, S., & Yang, H. (2009). Assessing the impact of climate  
545 change on water resources in Iran. *Water Resources Research*, 45, W10434, doi:10.1029/2008WR007615.

546 Ardakani, R. (2009). Overview of Water Management in Iran. *Proceeding of Regional Center on Urban Water*  
547 *Management*, Tehran, Iran.

548 Avsar, N.B., & Ustun, A. (2012). Analysis of regional time-variable gravity using  
549 GRACE's 10-day solutions. *FIG Working Week 2012, Knowing to manage the territory,*  
550 *protect the environment, evaluate the cultural heritage*, Rome, Italy, 6-10 May 2012,  
551 [http://www.fig.net/pub/fig2012/papers/ts04b/TS04B\\_avsar\\_ustun\\_5724.pdf](http://www.fig.net/pub/fig2012/papers/ts04b/TS04B_avsar_ustun_5724.pdf). (accessed date: May 2013)

552 Awange, J.L., Fleming, K.M., Kuhn, M., Featherstone, W.E., Heck, B., & Anjasmara, I. (2011). On the  
553 suitability of the  $4^{\circ} \times 4^{\circ}$  GRACE mascon solutions for remote sensing Australian hydrology. *Remote Sensing*  
554 *of Environment*, 115, 864-875. doi: 10.1016/j.rse.2010.11.014.

555 Awange, J., Forootan, E., Kusche, J., Kiema, J.K.B., Omondi, P., Heck, B., Fleming, K., Ohanya, S., &  
556 Gonçalves, R.M. (2013). Understanding the decline of water storage across the Ramsar-lake Naivasha using  
557 satellite-based methods. *Advances in Water Resources*, 60, 7-23, doi:10.1016/j.advwatres.2013.07.002.

558 Bari-Abarghouei, H., Asadi-Zarch, M.A., Dastorani, M.T., Kousari, M.R., & Safari-Zarch, M. (2011). The  
559 survey of climatic drought trend in Iran. *Stochastic Environmental Research and Risk Assessment*, 25 (6),  
560 851-863. doi:10.1007/s00477-011-0491-7.

561 Baur, O., Kuhn, M., & Featherstone, W.E. (2013). Continental mass change from GRACE over 2002-2011 and  
562 its impact on sea level. *Journal of Geodesy*, 87 (2), 117-125. doi:10.1007/s00190-012-0583-2.

563 Becker, M., Llovel, W., Cazenave, A., Güntner, A., & Crétaux, J.-F. (2010). Recent hydrological behavior  
564 of the East African great lakes region inferred from GRACE, satellite altimetry and rainfall observations.  
565 *Comptes Rendus Geoscience*, 342(3), 223-233. <http://dx.doi.org/10.1016/j.crte.2009.12.010>.

566 Birkett, C.M. (1995). The global remote sensing of lakes, wetlands and rivers for hydrological and climate  
567 research, in *Geoscience and Remote Sensing Symposium, 1995. IGARSS 95. 'Quantitative Remote Sensing for*  
568 *Science and Applications'*, Vol 3, 1979-1981.

569 Cardoso J.F., & Souloumiac, A. (1993). Blind beamforming for non-Gaussian signals. In: *IEEE proceedings*,  
570 362370. doi:10.1.1.8.5684.

571 Chambers, D.P. (2006). Observing seasonal steric sea level variations with GRACE and satellite altimetry. *J*  
572 *Geophys Res*, 111, C03010, doi:10.1029/2005JC002914.

573 Cheng, M., & Tapley, B.D. (2004). Variations in the Earth's oblateness during the past 28 years. *J Geophys*  
574 *Res*, 109, B09402, doi:10.1029/2004JB003028.

575 Crétaux, J-F., Jelinski, W., Calmant, S., Kouraev, A., Vuglinski, V., Bergé Nguyen, M., Gennero, M-C., Nino,  
576 F., Abarca Del Rio, F., Cazenave, A., & Maisongrande, P. (2011). SOLS: A lake database to monitor in near  
577 real time water level and storage variations from remote sensing data. *Journal of Advanced Space Research*,  
578 1497-1507. doi:10.1016/j.asr.2011.01.004.

579 Duan, J., Shum, C.K., Guo, J., & Huang, Z. (2012). Uncovered spurious jumps in the GRACE atmospheric  
580 de-aliasing data: potential contamination of GRACE observed mass change. *Geophys. J. Int.*, 191, 83-87,  
581 doi:10.1111/j.1365-246X.2012.05640.x.

582 FAO. (2009). FAO Water Report 34.

583 Farrell, W. E., & Clark, J. A. (1976). On postglacial sea level. *Geophysical Journal of the Royal Astronomical*  
584 *Society*, 46(3), 647-667.

585 Famiglietti, J.S., Rodell, M. (2013). Water in the balance. *Science* 340 (6138), 1300-1301,  
586 doi:10.1126/science.1236460.

587 Fenoglio-Marc, L., Kusche, J., & Becker, M. (2006). Mass variation in the Mediterranean Sea from  
588 GRACE and its validation by altimetry, steric and hydrologic fields. *Geophysical Research Letters*, 33(19),  
589 doi:10.1029/2006GL026851.

590 Fenoglio-Marc, L., Rietbroek, R., Grayek, S., Becker, M., Kusche, J., & Stanev, E. (2012). *Water*  
591 *mass variation in the Mediterranean and Black Sea. Journal of Geodynamics*, 59-60, 168-182,  
592 <http://dx.doi.org/10.1016/j.jog.2012.04.001>.

593 Flechtner, F. (2007a). AOD1B product description document for product releases 01 to 04. Technical Report,  
594 Geoforschungszentrum (GFZ), Potsdam.

595 Flechtner, F. (2007b). GFZ Level-2 processing standards document for level-2 product release 0004, GRACE  
596 327-743, Rev. 1.0. Technical Report, Geoforschungszentrum, Potsdam.

597 Forootan, E., Awange, J., Kusche, J., Heck, B., & Eicker, A. (2012). Independent patterns of water mass  
598 anomalies over Australia from satellite data and models. *Remote Sensing of Environment*, 124, 427-443,  
599 doi:10.1016/j.rse.2012.05.023.

- 600 Forootan, E., & Kusche, J. (2013). Separation of deterministic signals, using independent component analysis  
601 (ICA). *Stud. Geophys. Geod.*, Vol.57 (1), 17-26, doi: 10.1007/s11200-012-0718-1.
- 602 Forootan, E., & Kusche, J. (2012). Separation of global time-variable gravity signals into maximally indepen-  
603 dent components. *Journal of Geodesy*, 86 (7), 477-497, doi:10.1007/s00190-011-0532-5.
- 604 Forootan, E., Didova, O., Kusche, J., & Löcher, A. (2013). Comparisons of atmospheric data and reduction  
605 methods for the analysis of satellite gravimetry observations. *JGR-Solid Earth*, doi: 10.1002/jgrb.50160.
- 606 Frappart, F., Ramillien, G., Leblanc, M., Tweed, S.O., Bonnet, M.P., & Maisongrande, P. (2010). An independ-  
607 ent component analysis filtering approach for estimating continental hydrology in the GRACE gravity data.  
608 *Remote Sens Environ*, 115(1), 187-204. doi:10.1016/j.rse.2010.08.017
- 609 Ghandhari, A., & Alavi-Moghaddam, S.M.R. (2011). Water balance principles: A review of studies on five  
610 watersheds in Iran. *Journal of Environmental Science and Technology*, 4 (5), 465-479, ISSN: 1994-7887,  
611 doi:10.3923/jest.2011.465.479.
- 612 Grippa, M., Kergoat, L., Frappart, F., Araud, Q., Boone, A., de Rosnay, P., Lemoine, J.-M., Gascoin, S.,  
613 Balsamo, G., Ottlé, C., Decharme, B., Saux-Picart, S., & Ramillien, G. (2011). Land water storage variability  
614 over West Africa estimated by Gravity Recovery and Climate Experiment (GRACE) and land surface models.  
615 *Water Resour. Res.*, 47, W05549, doi:10.1029/2009WR008856.
- 616 Güntner, A., Stuck, J., Werth, S., Döll, P., Verzano, K., & Merz, B. (2007). A global analysis of temporal and  
617 spatial variations in continental water storage. *Water Resour. Res.*, 43, W05416, doi:10.1029/2006WR005247.
- 618 Güntner, A. (2008). Improvement of global hydrological models using GRACE data, *Surv. Geophys.*, 29, 375-  
619 397.
- 620 Ishii, M., & Kimoto, M. (2009). Reevaluation of historical ocean heat content variations with time-varying  
621 XBT and MBT depth bias corrections. *Journal of Oceanography* 65, 287-299.
- 622 Jekeli, C. (1981). Alternative methods to smooth the Earth's gravity field. Technical report rep 327. Depart-  
623 ment of Geodesy and Science and Surveying, Ohio State University, Columbus.
- 624 Jensen, L., Rietbroek, R., & Kusche, J. (2013). Land water contribution to sea level from GRACE and Jason-1  
625 measurements. *Journal of Geophysical Research-Oceans*, 118 (1), 212226, doi:10.1002/jgrc.20058.
- 626 Jiménez-Martínez, J., Longuevergne, L., Le Borgne, T., Davy, P., Russian, A., & Bour, O. (2013). Temporal  
627 and spatial scaling of hydraulic response to recharge in fractured aquifers: Insights from a frequency domain  
628 analysis. *WATER RESOURCES RESEARCH*, 49, 1-17, doi:10.1002/wrcr.20260.
- 629 Kampf, J., & Sadrinasab, M. (2006). The circulation of the Persian Gulf: a numerical study. *Ocean Sci.*, 2,  
630 27-41. <http://www.ocean-sci.net/2/27/2006/os-2-27-2006.html>.
- 631 Klees, R., Revtova, E.A., Gunter, B.C., Ditmar, P., Oudman, E., Winsemius, H.C. & Savenije, H.H.G. (2008).  
632 The design of an optimal filter for monthly GRACE gravity models. *Geophysical Journal International*, 175(2),  
633 417-432, doi:10.1111/j.1365-246X.2008.03922.x.
- 634 Klees, R., Zapreeva, E.A., Winsemius, H.C., & Savenije, H.H.G. (2007). The bias in GRACE estimates of  
635 continental water storage variations. *Hydrology and Earth System Sciences Discussions*, 11, 1227-1241.
- 636 Koch, K.R. (1988). Parameter estimation and hypothesis testing in linear models. Springer, New York.  
637 ISBN:978354065257.
- 638 Kosarev, A.N., & Yablonskaya, E.A., (1994). The Caspian Sea. The Netherlands:SPB Academic Publishing,  
639 pp. 260, ISBN-10:9051030886.
- 640 Kouraev, A.V., Crétaux, J.-F., Lebedev, S.A., Kostianov, A.G., Ginzburg, A.I., Sheremet, N.A., Mamedov,  
641 R., Zakharova, E.A., Roblou, L., Lyard, F., Calmant, S., & Berge-Nguyen, M. (2011). Satellite altimetry  
642 applications in the Caspian Sea (Chapter 13). In *Coastal Altimetry*, (Eds) S., Kostianov, A., Cipollini, P., and  
643 Benveniste, J. Springer, 331-366, ISBN:978-3-642-12795-3.
- 644 Kusche, J. (2007). Approximate decorrelation and non-isotropic smoothing of time-variable GRACE-type grav-  
645 ity field models. *Journal of Geodesy*, 81, 733-749, doi:10.1007/s00190-007-0143-3.
- 646 Kusche, J., Klemann, V., & Bosch, W. (2012). Mass distribution and mass transport in the Earth system.  
647 *Journal of Geodynamics*, 59-60, 1-8. <http://dx.doi.org/10.1016/j.jog.2012.03.003>.
- 648 Kusche, J., Schmidt, R., Petrovic, S., & Rietbroek, R. (2009). Decorrelated GRACE time-variable grav-  
649 ity solutions by GFZ, and their validation using a hydrological model. *Journal of Geodesy*, 83, 903-913,  
650 doi:10.1007/s00190-009-0308-3.
- 651 Lambeck, K., Esat, T.M., & Potter, E.K. (2002). Links between climate and sea levels for the past three million  
652 years. *Nature*, 2002 Sep 12, 419(6903), 199-206.
- 653 Lovel, W., Becker, M., Cazenave, A., Crétaux, J.-F., & Ramillien, G. (2010). Global land water storage  
654 change from GRACE over 2002-2009; Inference on sea level. *Comptes Rendus Geoscience*, 342, (3), 179-188,  
655 doi:<http://dx.doi.org/10.1016/j.crte.2009.12.004>.
- 656 Longuevergne, L., Scanlon, B.R., & Wilson, C.R. (2010). GRACE Hydrological estimates for small basins: Eval-  
657 uating processing approaches on the High Plains Aquifer, USA. *Water Resources Research*, 46 (11), W11517,  
658 doi:10.1029/2009WR008564.



659 [Longueveergne, L., Wilson, C.R., Scanlon, B.R., & Crétau, J-F. \(2012\). GRACE water storage estimates for](#)  
660 [the Middle East and other regions with significant reservoir and lake storage. \*Hydrol. Earth Syst. Sci. Discuss.\*,](#)  
661 [9, 11131-11159, doi:10.5194/hessd-9-11131-2012.](#)

662 [Modarres, R. \(2006\). Regional precipitation climates of Iran. \*Journal of Hydrology \(NZ\)\* 45 \(1\), 13-27,](#)  
663 [ISSN:0022-1708.](#)

664 [Mohammadi-Ghaleni, M., & Ebrahimi, K. \(2011\). Assessing impact of irrigation and drainage network on](#)  
665 [surface and groundwater resources - case study: Saveh Plain, Iran. ICID 21'st International Congress on](#)  
666 [Irrigation and Drainage, 15-23 October 2011, Tehran, Iran.](#)

667 [Motagh, M., Walter, T. R., Sharifi, M. A., Fielding, E., Schenk, A., Anderssohn, J., & Zschau, J. \(2008\). Land](#)  
668 [subsidence in Iran caused by widespread water reservoir overexploitation. \*Geophysical Research Letters\*, 35,](#)  
669 [L16403, doi:10.1029/2008GL033814.](#)

670 [Noory H., van der Zee, S.E.A.T.M., Liaghat, A.-M., Parsinejad, M., & van Dam, J.C. \(2011\). Dis-](#)  
671 [tributed agro-hydrological modeling with SWAP to improve water and salt management of the Voshm-](#)  
672 [gir irrigation and drainage network in Northern Iran. \*Agricultural Water Management\*, 98, 1062-1070,](#)  
673 [doi:10.1016/j.agwat.2011.01.013.](#)

674 [Pous, S.P., Carton, X., & Lazure, P. \(2004\). Hydrology and circulation in the Strait of Hormuz and the Gulf](#)  
675 [of Oman, Results from the GOP99 Experiment: 2. Gulf of Oman. \*Journal of Geophysical Research\*, 109,](#)  
676 [C12038, doi:10.1029/2003JC002146.](#)

677 [Preisendorfer, R. \(1988\). Principal component analysis in Meteorology and Oceanography. Elsevier: Amster-](#)  
678 [dam, 426 pages. ISBN:044430148.](#)

679 [Ramillien, G., Famiglietti, J.S., & Wahr, J. \(2008\). Detection of continental hydrology and glaciology signals](#)  
680 [from GRACE: a review. \*Surv. Geophys.\*, 29, 361-374, doi:10.1007/s10712-008-9048-9.](#)

681 [Reynolds, R.W., Rayne, N.A., Smith, T.M., Stokes, D.C., & Wang, W. \(2002\). An improved in situ and satellite](#)  
682 [SST analysis for climate. \*J. Clim.\*, 15 \(2002\), pp. 1609-1625.](#)

683 [Rietbroek, R., Brunnabend, S.E., Dahle, C., Kusche, J., Flechtner, F., Schröter, J., & Timmermann, R. \(2009\).](#)  
684 [Changes in total ocean mass derived from GRACE, GPS, and ocean modeling with weekly resolution. \*J Geophys\*](#)  
685 [Res., 114, C11004, doi:10.1029/2009JC005449.](#)

686 [Rietbroek, R., Brunnabend, S.E., Kusche, J., & Schröter, J. \(2012\). Resolving sea level contributions](#)  
687 [by identifying fingerprints in time-variable gravity and altimetry. \*Journal of Geodynamics\*, 59, 72-81,](#)  
688 [http://dx.doi.org/10.1016/j.jog.2011.06.007.](#)

689 [Rodell, M., Chen, J., Kato, H., Famiglietti, J., Nigro, J., & Wilson, C. \(2007\). Estimating ground water storage](#)  
690 [changes in the Mississippi River basin \(USA\) using GRACE. \*Hydrogeol. J.\* 15 159-166. doi:10.1007/s10040-006-](#)  
691 [0103-7.](#)

692 [Rodell, M., & Famiglietti, J.S. \(2001\). An analysis of terrestrial water storage variations in Illinois with](#)  
693 [implications for the Gravity Recovery and Climate Experiment \(GRACE\). \*Water Resour. Res.\*, 37\(5\), 1327-](#)  
694 [1340, doi:10.1029/2000WR900306.](#)

695 [Rodell, M., Houser, P.R., Jambor, U., Gottschalk, J., Mitchell, K., Meng, K., Arsenault, C.-J., Cosgrove, B.,](#)  
696 [Radakovich, J., Bosilovich, M., Entin, J.K., Walker, J.P., Lohmann, D., & Toll, D. \(2004\). The Global Land](#)  
697 [Data Assimilation System. \*Bulletin of the American Meteorological Society\*, 85 \(3\), 381-394.](#)

698 [Rodell, M., Velicogna, I., & Famiglietti, J.S. \(2009\). Satellite-based estimates of groundwater depletion in](#)  
699 [India. \*Nature\*, 460, 999-1002, doi:10.1038/nature08238.](#)

700 [Sarraf, M., Owaygen, M., Ruta, G., & Croitoru, L. \(2005\). Islamic Republic of Iran: Cost assessment of](#)  
701 [environmental degradation, Tech. Rep. 32043-IR, World Bank, Washington, D. C.](#)

702 [Schmeer, M., Schmidt, M., Bosch, W., & Seitz, F. \(2012\). Separation of mass signals within GRACE monthly](#)  
703 [gravity field models by means of empirical orthogonal functions. \*Journal of Geodynamics\*, 59-60, 124-132,](#)  
704 [doi:10.1016/j.jog.2012.03.001.](#)

705 [Schmidt, M., Seitz, F., & Shum, C.K. \(2008\). Regional fourdimensional hydrological mass variations](#)  
706 [from GRACE, atmospheric flux convergence, and river gauge data. \*J. Geophys. Res.\*, 113, B10402,](#)  
707 [doi:10.1029/2008JB005575.](#)

708 [Schnitzer, S., Seitz, F., Eicker, A., Güntner, A., Wattenbach, M., & Menzel, A. \(2013\). Estimation of soil loss](#)  
709 [by water erosion in the Chinese Loess Plateau using universal soil loss equation and GRACE. \*Geophys. J. Int.\*,](#)  
710 [doi:10.1093/gji/ggt023.](#)

711 [Sharifi, M.A., Forootan, E., Nikkhoo, M., Awange, J., & Najafi-Alamdari, M. \(2013\). A point-wise least](#)  
712 [squares spectral analysis \(LSSA\) of the Caspian Sea level fluctuations, using TOPEX/Poseidon and Jason-1](#)  
713 [observations. \*Advances in Space Research\*, 51 \(5\), 858-873. http://dx.doi.org/10.1016/j.asr.2012.10.001.](#)

714 [Shean, M. \(2008\). IRAN: 2008/09 wheat production declines due to drought.](#)  
715 [Commodity intelligence report. United States Department of Agriculture \(USDA\),](#)  
716 [http://www.pecad.fas.usda.gov/highlights/2008/05/Iran\\_may2008.html. Access date: 20.02.2013.](#)

717 [Shum, C.K., Jun-Yi, G., Hossain, F., Duan, J., Alsdorf, D.E., Duan, X-J, Kuo, C-Y., Lee, K., Schmitt, M.,](#)  
718 [& Wang, L. \(2011\). Inter-annual Water Storage Changes in Asia from GRACE Data. In R. Lal et al. \(eds.\),](#)  
719 [Climate Change and Food Security in South Asia, doi:10.1007/978-90-481-9516-9\\_6.](#)

720 Swenson, S., & Wahr, J. (2002). Methods for inferring regional surface-mass anomalies from Gravity Recovery  
721 and Climate Experiment (GRACE) measurements of time-variable gravity. *Journal of Geophysical Research*,  
722 107 (B9), ETG 3-1 - 3-13, doi:10.1029/2001JB000576.

723 Swenson, S., & Wahr, J. (2006). Post-processing removal of correlated errors in GRACE data. *Geophys Res*  
724 *Let.*, 33, L08402, doi:10.1029/2005GL025285.

725 Swenson, S., & Wahr, J. (2007). Multi-sensor analysis of water storage variations of the Caspian Sea. *Geophys*  
726 *Res Let.*, 34, L16401, doi:10.1029/2007GL030733.

727 Syed, T.H., Famiglietti, J.S., Chen, J., Rodell, M., Seneviratne, S.I., Viterbo, P., & Wilson, C.R. (2005).  
728 Total basin discharge for the Amazon and Mississippi River basins from GRACE and a land-atmosphere water  
729 balance. *Geophys. Res. Let.*, 32, L24404, doi:10.1029/2005GL024851.

730 Syed, T.H., Famiglietti, J.S., Rodell, M., Chen, J., & Wilson, C.R. (2008). Analysis of terrestrial water storage  
731 changes from GRACE and GLDAS. *Water Resources Research*, 44, W02433, doi:10.1029/2006WR005779.

732 Tapley, B., Bettadpur, S., Ries, J., Thompson, P., & Watkins, M. (2004a). GRACE measurements of mass  
733 variability in the Earth system. *Science*, 305, 503-505. <http://dx.doi.org/10.1126/science.1099192>.

734 Tapley, B., Bettadpur, S., Watkins, M., & Reigber, C. (2004b). The gravity recovery and cli-  
735 mate experiment: Mission overview and early results. *Geophysical Research Letters*, 31, L09607.  
736 <http://dx.doi.org/10.1029/2004GL019920>.

737 Van Camp, M., Radfar, M., Martens, K., & Walraevens, K. (2012). Analysis of the groundwater resource  
738 decline in an intramountain aquifer system in Central Iran. *GEOLOGICA BELGICA* (2012) 15/3: 176-180.

739 van Dijk, A.I.J.M. (2011) Model-data fusion: using observations to understand and reduce uncertainty in hy-  
740 drological models. 19th International Congress on Modelling and Simulation, Perth, Australia, 12-16 December  
741 2011. <http://mssanz.org.au/modsim2011/index.html>

742 van Dijk, A.I.J.M., Renzullo, L.J., & Rodell, M. (2011). Use of Gravity Recovery and Climate Experiment  
743 terrestrial water storage retrievals to evaluate model estimates by the Australian water resources assessment  
744 system. *Water Resour. Res.*, 47, W11524, doi:10.1029/2011WR010714.

745 Voss, K.A., Famiglietti, J.S., Lo, M-H., de Linage, C., Rodell, M., & Swenson, S.C. (2013). Groundwater  
746 depletion in the Middle East from GRACE with implications for transboundary water management in the  
747 Tigris-Euphrates-Western Iran region, *Water Resour. Res.*, 49, doi:10.1002/wrcr.20078.

748 Wahr, J., Molenaar, M., & Bryan, F. (1998). Time variability of the Earth's gravity field: Hydrological and  
749 oceanic effects and their possible detection using GRACE. *Journal of Geophysical Research* 103 (B12), 30205-  
750 30229, doi:10.1029/98JB02844.

751 Wahr, J., Swenson, S., Velicogna, I., & Zlotnicki, V. (2004). Time-variable gravity from GRACE: First results,  
752 *Geophysical Research Letters* paper 10.1029/2004GL019779.

753 Werth, S., Güntner, A., Schmidt, R., & Kusche, J. (2009). Evaluation of GRACE filter tools from a hy-  
754 drological perspective. *Geophysical Journal International*, 179, 1499-1515, [http://dx.doi.org/10.1111/j.1365-](http://dx.doi.org/10.1111/j.1365-246X.2009.04355.x)  
755 [246X.2009.04355.x](http://dx.doi.org/10.1111/j.1365-246X.2009.04355.x).

756 **Appendix A**

757 *Extracting Independent Components from GLDAS and Altimetry WS Changes*

758 ICA is applied on the data sets on each GLDAS and altimetry data sets  
759 using Eqs. 2 and 3 (see the details of application in e.g., Forootan and Kusche,  
760 2012). For altimetry products, ICA was individually implemented on (i) the  
761 Caspian Sea, (ii) the Persian and Oman Gulfs, (iii) the Aral Sea, and finally  
762 (iv) the other small lakes. The results are depicted in Figs. A1, A2, A3 and A4.  
763 Note that, similar to the main text, all the temporally independent components  
764 (ICs) are unit-less and the spatial patterns are given in millimeters.

765 Fig. A1 shows the first two independent modes, accounting for 93% of the  
766 surface WS variance in the Caspian Sea. The remaining 7% of the variance  
767 are noisy and are not shown here. IC1 shows an annual behaviour along with  
768 two linear trends, one from January 2002 to December 2005 with a rate of 108  
769  $mm/yr$  and the other from January 2006 to October 2008 with a rate of -152  
770  $mm/yr$ . IC2 indicates the main inter-annual variability from which, the spatial  
771 pattern of IC2 shows that the northern part of Caspian exhibits stronger inter-  
772 annual variations compared to the central and southern parts (see Fig. A1).  
773 This can be related to the climatic extremes, which are more pronounced in the  
774 northern part of the Caspian sea inducing stronger mass variations (Kouraev et  
775 al., 2011; Sharifi et al., 2013).

776 The ICA decomposition of WS changes of the Persian and Oman Gulfs also  
777 shows two significant components explaining 89% of the total variance. IC1  
778 shows an annual behaviour with a dipole spatial structure over the two gulfs  
779 (see Fig. A2, spatial pattern of IC1). IC2 shows a superposition of inter-annual  
780 variability and a positive linear trend ( $9 mm/yr$ ) dominant mainly over the  
781 head of the Persian Gulf, where Lambeck et al. (2002) reported a rise due to  
782 the post glacial rebound.

783 Fig. A3 shows that only one of the independent component of surface WS  
784 changes (corresponding to 89% of the total variance) over the Aral Sea is sta-  
785 tistically significant. IC1 of Aral shows the shrinking of the sea with an average  
786 linear rate of  $300 mm/yr$ . Results of ICA, applied on surface WS changes of  
787 the small lakes and reservoirs, are shown in Fig. A4. While only the first IC  
788 corresponding to 93% of total variance was significant, it shows that most of  
789 the surface water of Iran, specifically after the year 2005, are losing water. This  
790 situation might be related to the long-term drought condition of the country,  
791 see e.g. Bari-Abarghouei et al. (2011).

792 For brevity we only present the first two independent components of GLDAS  
793 data, explaining 71% of the total variance of terrestrial WS changes in Fig. A5.  
794 The temporal pattern of IC1 shows the dominant annual variation, while the  
795 spatial pattern of IC1 is mainly concentrated over north and west Iran. The  
796 temporal pattern of IC2 shows an overall linear trend (during 2002 to 2010)  
797 corresponding to a decrease of WS over the Markazi and Urmia Basins (see  
798 Fig. A5, spatial pattern of IC2). The derived trend appears to differ from the  
799 observations of WS changes, e.g., over Urmia (Fig. 3,A) and other small lakes  
800 (Fig. A4), where the WS decrease starts from 2005.

801 We should mention here, that to reconstruct 90% of the GLDAS data, one  
802 needs to select at least the first six independent components of GLDAS. The  
803 temporal behaviours of the remaining four independent components of GLDAS  
804 were difficult to interpret and are therefore not plotted. These components were,  
805 however, still used in the adjustment procedure.

## 806 **Appendix B**

### 807 *Self-gravitational Impact*

808 The strong seasonal mass fluctuations in the Caspian Sea will cause a time  
809 variable change in the geoid. On very short time scales (typically days), the  
810 ocean will adapt itself to this new equipotential surface, similar to the tidal  
811 response of the ocean. This implies that the sea level in the Gulfs and the  
812 Black Sea are (indirectly) influenced by the variations in the Caspian Sea. This  
813 effect is known as the self-consistent sea level response and has already been  
814 described in Farrel and Clarke (1976). When unaccounted for, this effect may  
815 potentially mix signal between the base-functions discussed in the main text.  
816 We, therefore, quantified its magnitude by taking the steric corrected sea level  
817 from altimetry and computed the self consistent sea level response according  
818 to Rietbroek et al. (2012). Fig. B1 shows the RMS of this effect. The effect  
819 is strongest in the Black Sea, since it is located closest to the Caspian Sea.  
820 However the magnitude of the effect is very small compared to the hydrological  
821 and oceanic signal sought such that it is not expected to influence the results.  
822

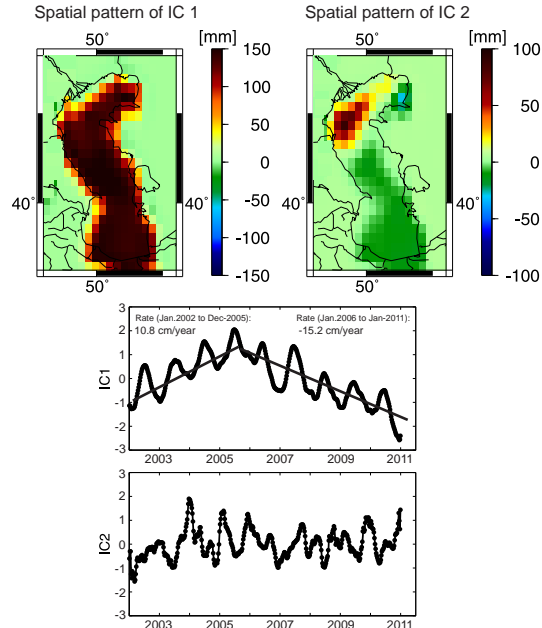


Figure A1: Results of the ICA method applied to the steric corrected SSH data (surface WS changes) over the Caspian Sea. The results are ordered according to their signal strength.

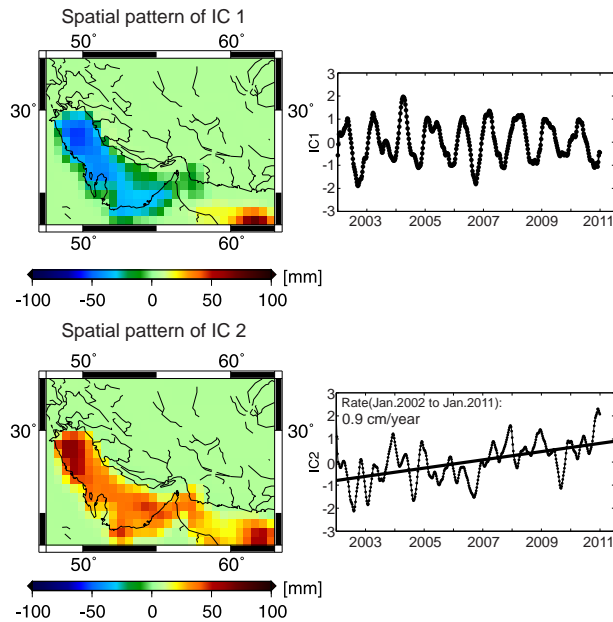


Figure A2: Results of the ICA method applied to the steric corrected SSH data (surface WS changes) over the Persian and Oman Gulfs. The results are ordered according to their signal strength.

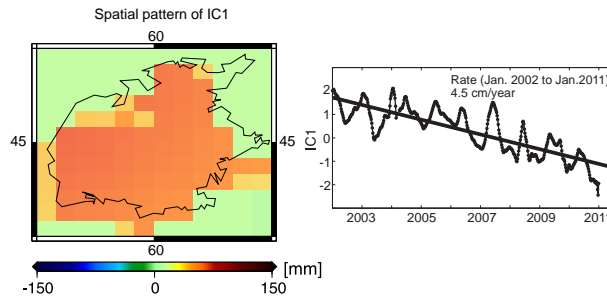


Figure A3: The dominant independent mode of surface WS changes of the Aral Sea.

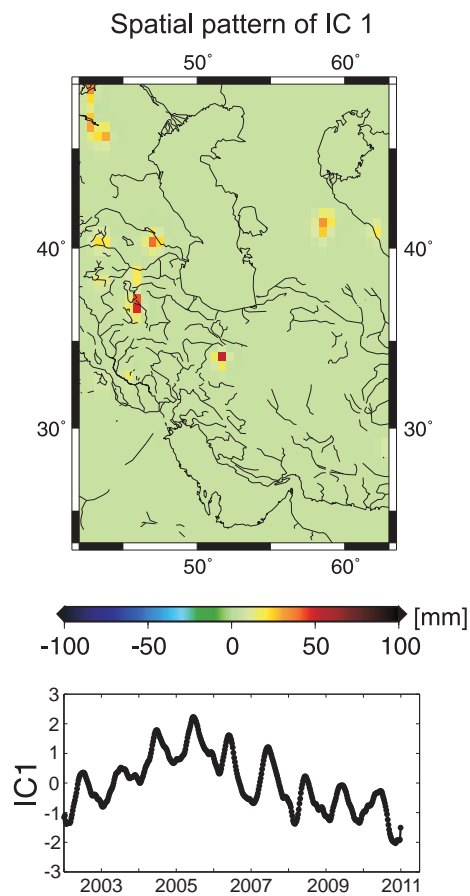


Figure A4: Results of the ICA method applied to the surface WS data over small lakes and reservoirs of the region.

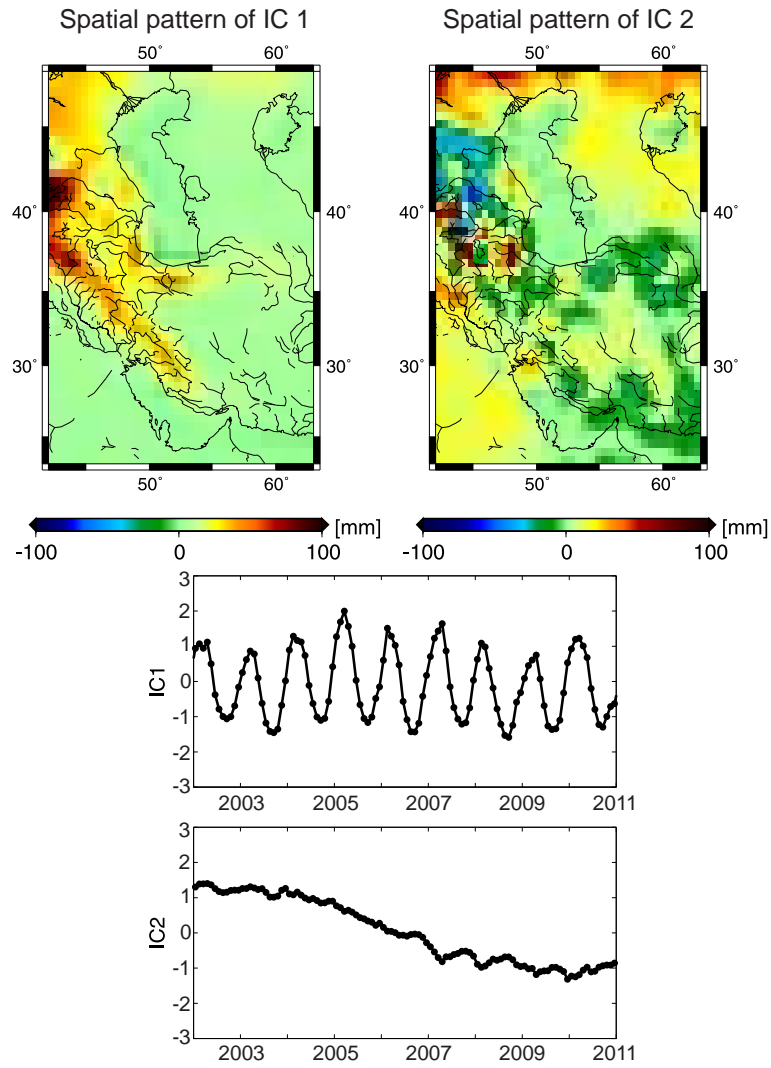


Figure A5: Results of the ICA method applied to the terrestrial WS outputs of the GLDAS model over a rectangular region, including Iran. The components are ordered according to the magnitude of variance they represent.



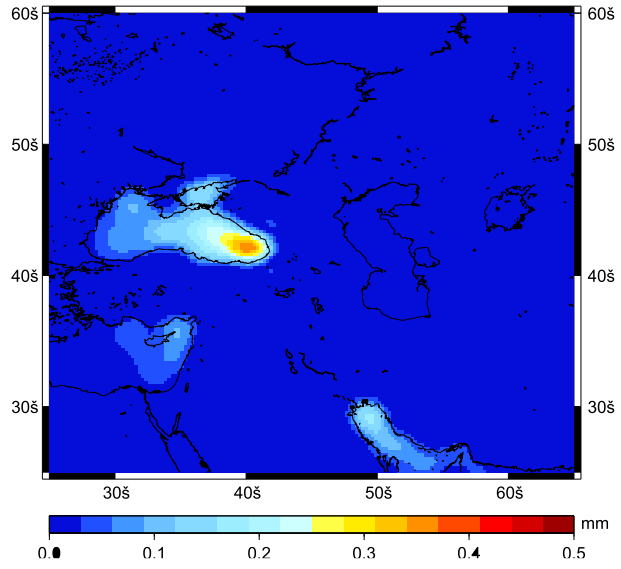


Figure B1: RMS of the self gravitational effect of the Caspian Sea's level variations (steric corrected altimetry) on relative sea level in the Gulfs and the Black Sea.